Surface-Micromachined 2-D Optical Scanners with High-Performance Single-Crystalline Silicon Micromirrors

Guo-Dung J. Su, *Student Member, IEEE,* Hiroshi Toshiyoshi, *Member, IEEE,* and Ming C. Wu, *Senior Member, IEEE*

***Abstract*—We have developed a novel batch-fabrication single-crystalline silicon micromirror bonding process to fabricate optically flat micromirror on polysilicon surface-micromachined two-dimensional (2-D) scanners. The electrostatically actuated 2-D scanner has a mirror area of 460 μm × 460 μm and an optical scan angle of ±7.5°. Compared with micromirror made by standard polysilicon surface-micromachining process, the radius of curvature of the micromirror has been improved by 150 times from 1.8 to 265 cm, with surface roughness $<$10 nm.**

***Index Terms*—Bonding, deep reactive ion etching, microelectromechanical devices, micromirrors, optical scanners, silicon-on-insulator.**

MICROELECTROMECHANICAL systems (MEMS) have emerged as one of the most promising technologies to fabricate microoptical devices such as switches [1], [2] and scanners [3]–[5]. The surface-micromachining technique is particularly attractive because of its versatility [6] and its potential integrability with complementary metal–oxide–semiconductor (CMOS) circuit process [7]. However, the micromirrors fabricated by the standard polysilicon surface-micromachining process (e.g., Multi-User MEMS Process, or MUMPs, offered by CRONOS) exhibit significant curvature due to residual stress of the deposited thin films [8], [9]. Furthermore, the surface topology is often affected by structures underneath the micromirror [10], [22]. For most applications, flat micromirrors with radius of curvature $>$30 cm and surface roughness $< \lambda/10$ are desired [11].

Though surface topology can be improved by careful layout design [10], [22] or adding a CMP process [12], the micromirrors are still subject to the residual stress and stress gradient. Meanwhile, silicon-on-insulator (SOI) has become popular material in bulk micromachining to fabricate MEMS devices because it simplifies the fabrication process and results in a very flat mirror surface [13]. Furthermore, SOI has been successfully integrated with surface micromachined scanners to improve the flatness of micromirrors [14].

We have developed a novel hybrid bulk/surface-micromachining process to fabricate high-performance micromirror on MUMPs chips. The micromirrors are formed on thick ($>$10 μm) SOI and then bonded to surface-micromachined actuators. This batch-fabrication process takes advantages of the flatness achievable with single crystalline silicon micromirrors without sacrificing the design flexibility of the standard polysilicon surface-micromachining process. We used AZ4620 photoresist for our adhesive bonding process because it can be easily patterned for selective area bonding and its ability to form void-free bonding [15]. In this letter, we describe the fabrication and the performance of the MEMS 2-D scanners with bonded micromirrors. Optical scanners with large (460 μm × 460 μm) and flat (radius of curvature $>$265 cm, surface roughness $<$10 nm) micromirrors have been successfully demonstrated.

The deformation of the micromirror fabricated by standard polysilicon surface-micromachining technology is caused by residual stress and stress-gradient in the thin-film deposition processes. More insight on the factors affecting the flatness of micromirrors can be obtained by examining the analytical expression of 1-D structures [9]

$$\delta|_{\xi=(L/2)} = \frac{\boldsymbol{M}}{\boldsymbol{P}}\left[\sec\left(\frac{\boldsymbol{kL}}{2}\right) - 1\right],$$
$$k = \sqrt{\frac{P}{EI}} \quad \text{and} \quad I = \int_A z^2\, dA \tag{1}$$

where $\boldsymbol{E}$ is the Young's modulus, $\boldsymbol{I}$ is the moment of inertia, δ is the deflection, ξ is the direction variable, $\boldsymbol{L}$ is the length of the mirror, $\boldsymbol{z}$ is the mirror thickness and $\boldsymbol{A}$ and the cross-section area of the mirror, respectively, $\boldsymbol{P}$ is the reactive axial force and $\boldsymbol{M}$ is the bending moment, which are caused by residual stress and stress gradient, respectively. The equation shows that the deflection of the mirror can be reduced by increasing its thickness (larger $\boldsymbol{I}$) and reducing the bending moment (smaller $\boldsymbol{M}$). SOI is an ideal candidate for micromirror because it is free of internal stress and has smooth surface. Besides, SOI with a wide range of silicon layer thickness is available for making micromirrors.

The MEMS 2-D scanner used in this experiment is similar to that reported in [3]. It is fabricated by MUMPs. Fig. 1(a) shows the scanning electron micrograph (SEM) of the 2-D scanner. The polysilicon micromirror is attached to two nested rings by orthogonal folded springs. The 2-D scanner is realized by the self-assembled Micro-Elevator by Self-Assembly (MESA) [16] structures, which raise the polysilicon mirror to 60 μm above the substrate to increase the scanning angle. The self-assembly process is controlled by the integrated scratch drive actuators [17], and no manual intervention is necessary. Scanning of the micromirror is actuated electrostatically by the four split electrodes underneath the mirror.

Manuscript received September 19, 2000; revised February 28, 2001. This work was supported in part by the Defense Advanced Research Projects Agency (DARPA) under grant F30602-97-2-0122 and grant DAAH01-99-C-R220.

The authors are with the Electrical Engineering Department, University of California at Los Angeles, Los Angeles, CA 90034 USA.

Publisher Item Identifier S 1041-1135(01)04569-4.

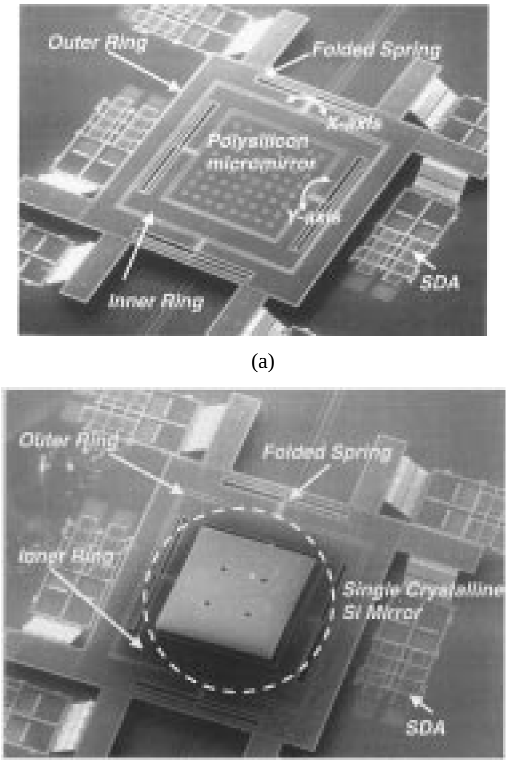

(a)

(b)

Fig. 1. SEM pictures of assembled 2-D scanner with (a) polysilicon mirror and (b) single crystalline Si mirror.

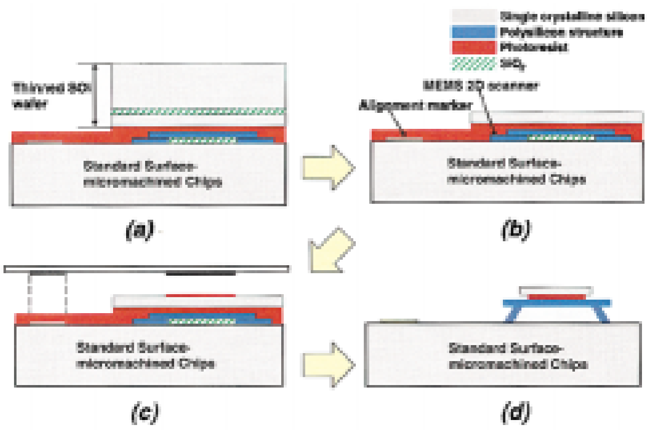

Fig. 2. Schematic drawing illustrating the mirror bonding process.

The SEM of the improved 2-D scanner with single-crystalline micromirror is shown in Fig. 1(b). The single-crystalline silicon mirror bonding process is described in Fig. 2. First, a thinned SOI wafer with 200-μm-thick substrate is flipped over and bonded to the MUMPs chips by photoresist (AZ 4620). The photoresist is spun over the entire chip and the bonded wafers are baked in a vacuum oven at 140 °C for 8 h. The SOI wafer is slightly smaller than the scanner chip so the alignment markers on the scanner chip can be utilized to align the micromirror. The substrate of the SOI wafer is then completely removed by deep reactive ion etching (DRIE), which stops at the buried oxide layer. The exposed area of the MUMPs chip is protected by the photoresist during DRIE etching. The 1-μm-thick buried oxide of the SOI wafer is etched away in 49% HF solution for 1 min, as shown in Fig. 2(b). The single crystalline silicon mirror is aligned to the polysilicon actuators by photolithography and then patterned by DRIE using photoresist as masks. After that, the remaining photoresist is cleaned by oxygen plasma and the chip is baked in the oven at 230 °C for 3 h to hard cure the photoresist underneath the single crystalline silicon mirror. It is then fully released in HF solution and rinsed in water and isopropanol alcohol; the MEMS 2-D scanner is assembled by the on-chip actuators.

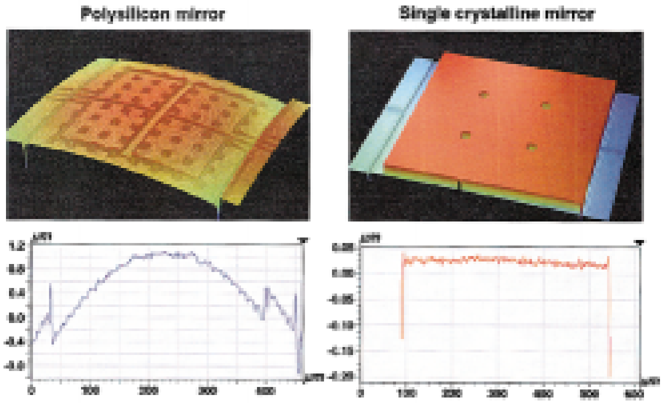

(a) (b)

Fig. 3. 3-D plot and cross section profile of (a) polysilicon mirror and (b) single crystalline Si mirror.

Fig. 3 shows the measured deformation of the thin-film polysilicon mirror and the single crystalline silicon mirror after they are released and assembled. The measurement is performed by an optical interferometric surface profiler. Using the first-order paraxial rays approximation [18], the radius of the curvature is calculated by the expression

$$\boldsymbol{R} = \frac{\boldsymbol{D}^2}{8\boldsymbol{x}} \tag{2}$$

where $\boldsymbol{R}$ is radius of curvature, $\boldsymbol{D}$ is the length of the mirror (460 μm in this experiment), and $\boldsymbol{x}$ is the deformation of the mirror from the center to the edge. The deformation of the polysilicon mirror is measured to be 1.45 μm in convex shape, which corresponds to a curvature of 1.8 cm. The micromirror consists of an oxide layer trapped between two polysilicon layers with a total thickness of 4.25 μm. On the other hand, the deformation of the single crystalline mirror is less than 10 nm, which corresponds a radius of curvature greater than 265 cm. The measured thickness of the single crystalline silicon is 22.5 μm.

The quality of the micromirrors is also examined optically. The experimental setup is shown in Fig. 4. The optical beam from a He–Ne laser is reduced by a telescope to 0.28 mm in diameter so it is completely covered by the micromirror. The profiles of the optical beam reflected from the micromirrors are recorded by a CCD camera. A neutral density filter is used to prevent CCD from saturation. As shown in Fig. 4, the optical quality of the single crystalline micromirror is better than that of the polysilicon micromirror. The full-width at half-maximum spot sizes of the beams reflected from the polysilicon and the single crystalline silicon mirror are 2.04 and 0.3 mm, respectively. That means that the number of resolvable spots for the

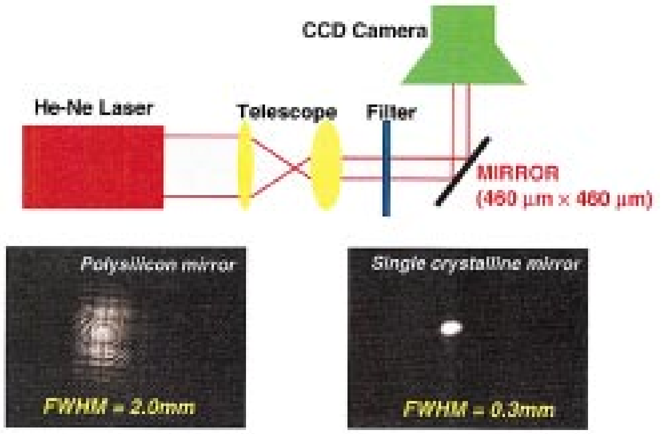

Fig. 4. Far-field distribution pattern of optical beam reflected from (a) polysilicon mirror and (b) single crystalline mirror for collimated input beams.

single crystalline mirror is about seven times better than that of the polysilicon mirror for the collimated beam. The maximum mechanical scan angles of both optical scanners are ±7.5°.

The bonding strength is measured by the pull-off method, which measures the force needed to separate two bonded pieces. Under the current bonding condition, the bonding strength is measured to be approximately 0.75 MPa (limited by the resolution of test equipment). This is slightly lower than (but comparable to) the bonding strengths reported for other adhesive bonding methods: 2–10 MPa for fluoropolymer bonding [19], 0–4 MPa for SiO_2–SiO_2 bonding [20], and 1.6 MPa for UV-epoxy [21]. Nevertheless, it is strong enough to survive the releasing and drying processes as well as normal operation of the scanner. The bonding quality depends critically on whether the interface is void-free or not. We perform the initial bonding process (140 °C for 8 h) in a vacuum oven to ensure removal of any trapped bubbles between the bonded surfaces. The amount of pressure applied during the bonding process is critical to the bonding strength. We applied a pressure 3 MPa through a weight placed on the sample. The final baking at 230 °C further enhances the bonding strength by resin crosslinking. The bonding method described in this letter is a batch processing technique. In principle, it can be extended to wafer-scale process. Indeed, it has been reported in [15] that void-free bonding can be achieved between two flat wafers using hard-baked photoresist. For bonding micromirrors to a nonplanar actuator wafer, such as the MUMPs wafer used in this letter, issues such as bonding uniformity and yield need to be addressed. It is beyond the scope of the letter, since our sample size is limited to chip scale by the foundry service.

In summary, we have successfully developed a novel bonding process to improve the quality of micromirrors in optical MEMS devices. MEMS 2-D optical scanners with bonded single crystalline Si micromirrors have been successfully demonstrated. A radius of curvature $>$265 cm, surface roughness $<$10 nm, and a maximum mechanical scan angle of ±7.5° have been achieved. Our new technique enables high-performance optical MEMS devices to be built using low-cost, widely accessible commercial surface-micromachining process.

REFERENCES

[1] R. T. Chen, H. Nguyen, and M. C. Wu, "A high-speed low-voltage stress-induced micromachined 2 × 2 optical switch," *IEEE Photon. Technol. Lett.*, vol. 11, pp. 1396–1398, Nov. 1999.

[2] D. T. Nelson, V. A. Aksyuk, S. Arney, N. R. Basavanhally, and C. R. Giles, "Fully provisioned 112 * 112 micro-mechanical optical crossconnect with 35.8 Tb/s demonstrated capacity," in *Proc. OFC 2000*, Baltimore, MD, Mar. 7–10, 2000, Postdeadline paper PD12.

[3] L. Fan and M. C. Wu, "Two-dimensional optical scanner with large angular rotation realized by self-assembled micro-elevator," presented at the Proc. IEEE LEOS Summer Topical Meeting on Optical MEMS, Monterey, CA, Aug. 20–22, 1998, Paper WB4.

[4] G. J. Su, S. S. Lee, and M. C. Wu, "Optical scanners realized by surface-micromachined vertical torsion mirror," *IEEE Photon. Technol. Lett.*, vol. 11, pp. 587–589, May 1999.

[5] M. Kiang, O. Solgaard, K. Lau, and R. S. Muller, "Electrostatic comb-drive-actuated micromirrors for laser-beam scanning and positioning," *J. Microelectromech. Syst.*, vol. 7, pp. 27–37, Mar. 1998.

[6] R. S. Muller and K. Lau, "Surface-micromachined microoptical elements and systems," *Proc. IEEE*, vol. 86, pp. 1705–1720, Aug. 1998.

[7] J. Smith, S. Montague, J. J. Sniegowski, J. R. Murray, and P. J. McWhorter, "Embedded micromechanical devices for the monolithic integration of MEMS with CMOS," in *IEDM Tech. Dig.*, Dec. 1995, pp. 609–612.

[8] P. M. Hagelin and O. Solgaard, "Optical raster-scanning displays based on surface-micromachined polysilicon mirrors," *IEEE J. Select. Topics Quantum Electron.*, vol. 5, pp. 67–74, Jan.–Feb. 1999.

[9] Y. Min and Y. Kim, "Modeling, design, fabrication and measurement of a single layer polysilicon micromirror with initial curvature compensation," *Sens. Actuators A, Phys.*, vol. A78, pp. 8–17, Nov. 1999.

[10] D. M. Burns and V. M. Bright, "Designs to improve polysilicon micromirror surface topology," in *Proc. SPIE-Int. Soc. Opt. Eng., Miniaturized systems with micro-optics and micromechanics II*, San Jose, CA, Feb. 10–12, 1997.

[11] G. J. Su, W. Piyawattanmethna, R. Rollier, L. Fan, and M. Wu, "MEMS 2D scanning mirror for dynamic alignment in optical interconnect," in *Proc. Integrated Photonic Research (IPR '99)*, Santa Barbara, CA, July 1999.

[12] R. Nasby, J. Sniegowski, J. Smith, S. Montague, C. Barron, W. Eaton, P. McWhorter, D. Hetherington, C. Apblett, and J. Fleming, "Application of chemical-mechanical polishing to planarization of surface-micromachined devices," in *Tech. Dig. Solid-State Sensor and Actuator Workshop*, 1996, pp. 48–53.

[13] K. Yamada and T. Kuriyama, "A novel asymmetric silicon micro-mirror for optical beam scanning display," in *An Investigation of Micro Structures, Sensors, Actuators, Machines and Systems*, Heidelberg, Germany, Jan. 25–29, 1999, pp. 110–115.

[14] J. Nee, R. Conat, M. Hart, R. Muller, and K. Lau, "Stretched-film micromirrors for improved optical flatness," in *Proc. IEEE MEMS 2000*, Miyazaki, Japan, Jan. 23–27, 2000, pp. 704–709.

[15] F. Niklaus, P. Enoksson, E. Kalvesten, and G. Stemme, "Void-free full wafer adhesive bonding," in *Proc. MEMS 2000 Conf.*, Miyazaki, Japan, pp. 247–252.

[16] L. Fan, M. Wu, K. Choquette, and M. Crawford, "Self-assembled microactuated XYZ stages for optical scanning and alignment," in *Proc. Int. Solid State Sensors and Actuators Conf. (Transducer '97)*, Chicago, IL, pp. 319–322.

[17] T. Akiyama and H. Fujita, *IEEE Micro Electro Mechanical System Workshop*, Amsterdam, The Netherlands, Jan.29–Feb. 2, 1995.

[18] B. Saleh and M. Teich, *Fundamentals of Photonics*. New York: Wiley, 1991.

[19] A. Han, K. W. Oh, S. Bhansali, H. T. Henderson, and C. H. Ahn, "A low temperature biochemically compatible bonding technique using fluoropolymers for biochemical microfluidic systems," in *Proc. 2000 MEMS Conf.*, Miyazaki, Japan, Jan. 23–27, 2000, pp. 414–418.

[20] H. Nakanishi, T. Nishimoto, R. Nakamura, A. Yotsumoto, and S. Shoji, "Studies on SiO_2-SiO_2 bonding with hydrofluoric acid-room temperature and low stress bonding technique for MEMS," in *Proc. 1998 MEMS Conf.*, Heidelberg, Germany, Jan. 25–29, 1998, pp. 609–614.

[21] H. Nguyen, P. Patterson, H. Toshiyoshi, and M. C. Wu, "A substrate-independent wafer transfer technique for surface-micromachined devices," in *Proc. 2000 MEMS Conf.*, Miyazaki, Japan, Jan. 23–27, 2000, pp. 628–632.

[22] D. M. Burns and V. M. Bright, "Designs to improve polysilicon micromirror surface topology," *Proc. SPIE-Int. Soc. Opt. Eng.*, pp. 100–110, 1997.